iScience

CellPress
OPEN ACCESS

Article

Mycobacterial Rv1804c binds to the PEST domain of IκBα and activates macrophage-mediated proinflammatory responses

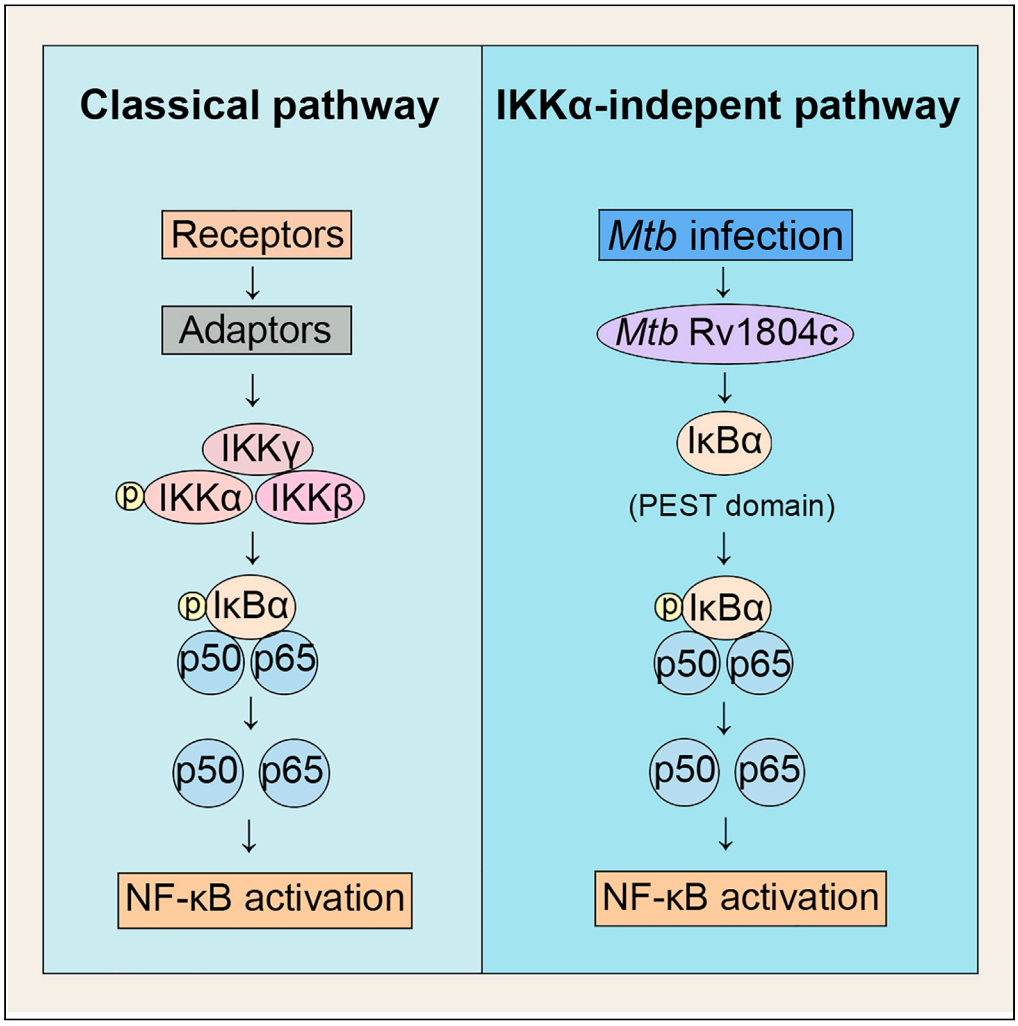

Jianjian Zheng, Chunsheng Dong, Sidong Xiong

chunshengdong@suda.edu.cn (C.D.)
sdxiong@suda.edu.cn (S.X.)

Highlights

Rv1804c activates IκBα by directly interacting with its PEST domain

Rv1804c activates proinflammatory responses in an IKKα-independent manner

Rv1804c inhibits mycobacterial survival both *in vitro* and *in vivo*

Rv1804c is enriched in attenuated but not in virulent mycobacteria

Zheng et al., iScience *27*, 109101
March 15, 2024 © 2024 The Author(s).
https://doi.org/10.1016/j.isci.2024.109101

iScience

CellPress
OPEN ACCESS

Article

Mycobacterial Rv1804c binds to the PEST domain of IκBα and activates macrophage-mediated proinflammatory responses

Jianjian Zheng,[1] Chunsheng Dong,[1,*] and Sidong Xiong[1,2,*]

SUMMARY

Recognition of the components of *Mycobacterium tuberculosis* (*Mtb*) by macrophages is vital for initiating a cascade of host immune responses. However, the recognition of *Mtb*-secretory proteins by the receptor-independent pathways of the host remains unclear. Rv1804c is a highly conserved secretory protein in *Mtb*. However, its exact function and underlying mechanism in *Mtb* infection remain poorly understood. In the present study, we observed that Rv1804c activates macrophage-mediated proinflammatory responses in an IKKα-independent manner. Furthermore, we noted that Rv1804c inhibits mycobacterial survival. By elucidating the underlying mechanisms, we observed that Rv1804c activates IκBα by directly interacting with its PEST domain. Moreover, Rv1804c was enriched in attenuated but not in virulent mycobacteria and associated with the disease process of tuberculosis. Our findings provide an alternative pathway via which a mycobacterial secretory protein activates macrophage-mediated proinflammatory responses. Our study findings may shed light on the prevention and treatment of tuberculosis.

INTRODUCTION

Tuberculosis (TB), caused by *Mycobacterium tuberculosis* (*Mtb*), is the oldest global epidemic since prehistoric times; it remains the leading cause of death, particularly in low-income countries.[1,2] The emergence of multidrug-resistant *Mtb*, human immunodeficiency virus coinfection, and the coronavirus disease 2019 pandemic has urgently warranted TB control.[3] Furthermore, developing new TB vaccines and therapies by comprehensively understanding the close interaction between *Mtb* and host immunity is vital.

First, the aerosolized *Mtb* reaches the lungs, where resident alveolar macrophages are the first cells to encounter *Mtb* infection.[4–6] The activation of pattern recognition receptors leads to various cellular events that contribute to anti-*Mtb* immunity in the host, including inflammatory responses, an intracellular homeostatic process in response to harmful stimuli, including *Mtb* infection.[7–10] A remarkable feature of intracellular *Mtb* infection is that a set of mycobacterial proteins are secreted into the cytoplasm of infected cells.[11] Many *Mtb* secretory proteins can modify intrinsic antimicrobial mechanisms in cells, including inflammatory responses, by targeting host receptors, cellular immune components, and the ubiquitin system. For example, *Mtb* early secreted antigenic target 6 kDa (ESAT-6) directly interacts with Toll-like receptor (TLR) 2 and inhibits the TLR signaling pathways in macrophages.[9] On the other hand, the *Mtb* protein tyrosine phosphatase A inhibits innate immunity by binding to the host ubiquitin system and dephosphorylating c-Jun N-terminal kinase (JNK) and p38.[12] Furthermore, *Mtb* PPE68 suppresses the tumor necrosis factor receptor (TNF)-associated factor 6 (TRAF6)-driven NF-κB and AP-1 signaling pathways by interacting with makorin ring finger protein 1.[13] *Mtb* Rv0222 suppresses the expression of proinflammatory cytokines by interacting with anaphase-promoting complex subunit 2, an E3 ubiquitin ligase, in the host.[14] *Mtb* PPE36 inhibits host inflammatory responses and increases bacterial loads in infected macrophages and mice by promoting E3 ligase smurf1-mediated MyD88 degradation.[15] *Mtb* MmsA induces DC activation by activating the MAPK and NF-κB signaling pathways.[16] In addition, some *Mtb*-associated secretory proteins activate immune responses in a host receptor-dependent pathway. For example, *Mtb* EsxL induces the activation of the NF-κB pathway in a TLR2- and IKK-dependent manner.[17] Taken together, although some secretory proteins have been identified as virulence factors that interfere with various host cell processes to promote *Mtb* survival, whether and how these secretory proteins are recognized by the receptor-independent pathways in the host to initiate immune responses remain largely unclear.

The characterization of protein-protein interactions (PPIs) using mass spectrometry is a powerful method for detecting complex biological systems in an unbiased manner.[18,19] In 2018, Bennett and colleagues used an affinity purification mass spectrometry approach to identify 187 PPIs between *Mtb* and humans. Of them, Rv1804c, a conserved hypothetical protein in *Mtb*, is a key molecule in the PPI network.[20] Some studies have reported that Rv1804c is a nonessential gene for the *in vitro* growth of *H37Rv* and may be linked to innate immunity and autophagy.[21,22] However, the exact function and potential mechanism of Rv1804c in *Mtb* infection remain poorly understood. In the present study, we elucidated that the *Mtb* secretory protein Rv1804c activates inflammatory responses in macrophages in an IKKα-independent manner.

[1]Jiangsu Key Laboratory of Infection and Immunity, Institutes of Biology and Medical Sciences, Soochow University, Suzhou 215123, China
[2]Lead contact
*Correspondence: chunshengdong@suda.edu.cn (C.D.), sdxiong@suda.edu.cn (S.X.)
https://doi.org/10.1016/j.isci.2024.109101

This is an open access article under the CC BY-NC-ND license (http://creativecommons.org/licenses/by-nc-nd/4.0/).

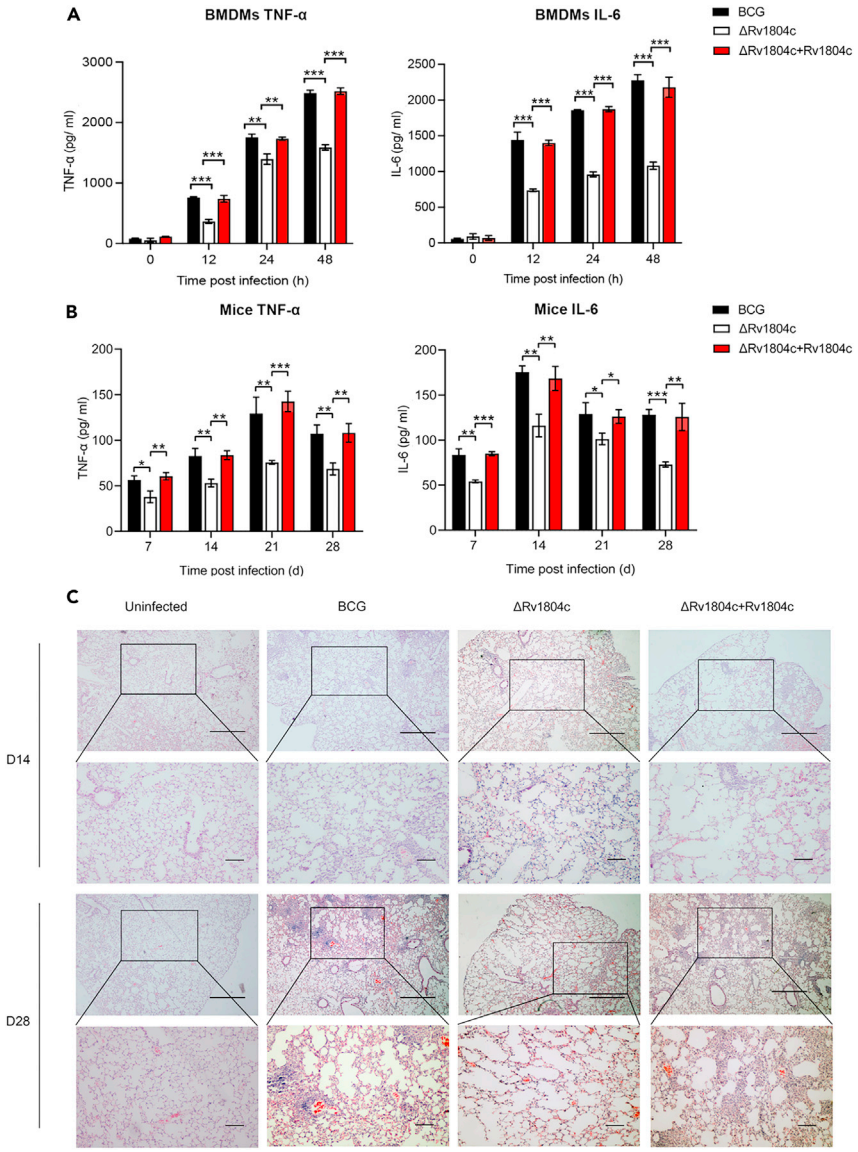

Figure 1. Rv1804c knockout in *BCG* suppresses inflammatory responses

(A) ELISA to quantify the levels of TNF-α and IL-6 in the supernatants of BMDMs infected with *BCG*, *ΔRv1804c*, and *ΔRv1804c+Rv1804c* at an MOI of 10 for 0, 8, 12, and 24 h.

(B) ELISA to quantify the levels of TNF-α and IL-6 in the lung tissues of mice infected with *BCG*, *ΔRv1804c*, and *ΔRv1804c+Rv1804c* (2×10^7 CFU/mice) for 7, 14, 21, and 28 days.

(C) Hematoxylin and eosin staining of the lung tissues of infected mice at 14 and 28 days post-infection. Scale bars: 1,000 μm (top; original magnification, ×40) and 200 μm (bottom; original magnification, ×100). Data are presented as means ± SD. *$p < 0.01$, **$p < 0.01$, and ***$p < 0.001$.

Furthermore, it increases the phosphorylation level of IκBα by interacting with the proline glutamate serine threonine (PEST) domain of IκBα, thereby enhancing subsequent IκBα ubiquitination and degradation. Our study findings highlight an alternative pathway via which *Mtb* secretory proteins can activate inflammatory responses.

RESULTS

Rv1804c knockout in *BCG* suppresses inflammatory responses and promotes mycobacterial survival

Macrophage-mediated inflammatory responses play a vital role in the survival of bacillus during *Mtb* infection. The cytokines tumor necrosis factor-alpha (TNF-α) and interleukin-6 (IL-6) participate in *Mtb* clearance by macrophages.[23] After performing NCBI protein BLAST, we identified that the protein sequence of *BCG*-derived Rv1804c is identical to that of *Mtb* Rv1804c. Herein we obtained the Rv1804c-deficient *BCG* strain (*ΔRv1804c*) and its complement strain (*ΔRv1804c+Rv1804c*) to explore the potential impact of Rv1804c on the macrophage

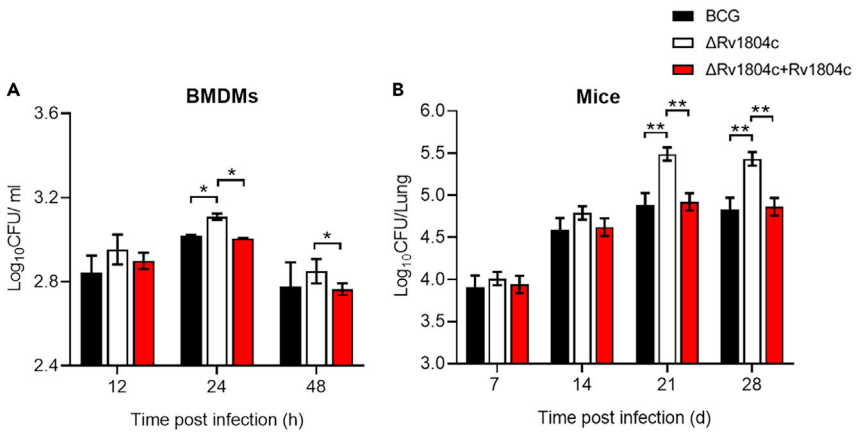

Figure 2. Rv1804c knockout in *BCG* promotes mycobacterial survival

(A) Colony-forming unit (CFU) assay of BMDMs infected with *BCG*, *ΔRv1804c*, and *ΔRv1804c+Rv1804c* at an MOI of 10 for 12, 24, and 48 h.

(B) CFU assay of the lung tissues of mice infected with *BCG*, *ΔRv1804c*, and *ΔRv1804c+Rv1804c* (2×10^7 CFU/mice) for 7, 14, 21, and 28 days. Data are presented as means ± SD. *p < 0.01, **p < 0.01.

inflammatory responses. Bone marrow-derived macrophages (BMDMs) and RAW264.7 cells were infected with *ΔRv1804c*, *ΔRv1804c+Rv1804c*, and control *BCG*. The levels of the inflammatory cytokines TNF-α and IL-6 were measured. qPCR (Figure S1A) and ELISA (Figure 1A) revealed that *ΔRv1804c*-infected BMDMs had significantly decreased inflammatory cytokine levels. Similar results were observed in RAW264.7 cells (Figures S1B and S1C). The mouse intranasal mycobacterial infection model was established using a previously described method.[15] We measured the inflammatory cytokine levels, pathological damage, and immune cells infiltration in the lungs of infected mice. Consistently, *ΔRv1804c*-infected mice had lower inflammatory cytokine levels in lungs as measured by qPCR (Figure S1D) and ELISA (Figure 1B). On days 14 and 28 post-challenge, compared with *ΔRv1804c+Rv1804c* and control *BCG* mice, an alleviative inflammatory response was observed in *ΔRv1804c*-infected mice (Figure 1C). It was evidenced with less immune cells infiltration, and much more intact alveolar space, suggesting that Rv1804c knockout in *BCG* alleviate pathological damage in the lung tissues of infected mice.

We then examined the effects of Rv1804c on bacterial survival. BMDMs and RAW264.7 cells were infected with *ΔRv1804c* and its control. The CFU assay was performed to determine the intracellular bacillary burden in infected cells and mice as previously described.[24] Compared with *ΔRv1804c+Rv1804c*, and control *BCG*, *ΔRv1804c* had a higher bacillary burden in infected BMDMs (Figure 2A) and RAW264.7 cells (Figure S1E). Next, to confirm the effects of Rv1804c on bacterial survival *in vivo*, C57BL/6 mice were intranasally infected with *ΔRv1804c*, *ΔRv1804c+Rv1804c*, and control *BCG*. The results demonstrated that *ΔRv1804c*, the *Rv1804c*-deficient strain, had a higher bacillary burden in the lung tissue of infected mice (Figure 2B). Taken together, these data indicate that Rv1804c knockout in *BCG* suppresses inflammatory responses and promotes bacterial survival *in vitro* and *in vivo*.

Exogenous Rv1804c expression in *Mycobacterium smegmatis* (*MS*) promotes inflammatory responses and inhibits mycobacterial survival

MS has been used as a model organism to study the molecular, physiological, and drug-resistant mechanisms of *Mtb*.[25] The *MS* genome does not encode the Rv1804c gene. In this study, to verify whether Rv1804c affects mycobacterial growth, a recombinant *MS* strain that exogenously expresses Rv1804c was generated. Western blotting revealed that Rv1804c was detected both in bacterial pellets and culture filtrates in *MS_Rv1804c* (Figure S2A) and *Mtb H37Rv* (Figure S2B), this indicates that Rv1804c is a secretory protein. Furthermore, the growth curve (Figure S2C) and XTT assay (Figure S2D) revealed that Rv1804c expression in *MS* did not affect bacterial growth in the culture medium.

Next, to evaluate the effect of Rv1804c on inflammatory responses during mycobacterial infection, BMDMs were infected with *MS_Rv1804c* and control *MS_WT*. The inflammatory cytokine levels (TNF-α and IL-6) were measured, with significantly increased inflammatory cytokine levels in *MS_Rv1804c*-infected BMDMs, as detected via qPCR (Figure S3A) and ELISA (Figure 3A). Similar results were observed in RAW264.7 cells (Figures S3B and S3C). Furthermore, compared with *MS_WT*-infected mice, *MS*_Rv1804c-infected mice had higher inflammatory cytokine levels in lungs (Figures 3B and S3D), higher immune cells infiltration, and much less intact alveolar space, on day 6 post-challenge (Figure 3C).

In contrast, Rv1804c exogenous expression in *MS* had a lower survival rate in BMDMs (Figure 4A) and RAW264.7 cells (Figure S3E) compared with control *MS_WT*. Consistently, the bacillary burden in the lung tissues of *MS_Rv1804c*-infected mice was significantly lower than that in those of *MS_WT*-infected mice (Figure 4B). Taken together, these data suggest that exogenous Rv1804c expression in *MS* promotes inflammatory responses and inhibits mycobacterial survival both *in vitro* and *in vivo*.

Rv1804c promotes inflammatory responses via the NF-κB pathway

Studies have comprehensively reported the function of NF-κB in inflammatory responses against *Mtb* infection.[26,27] Herein, to explore the mechanism by which Rv1804c promotes host inflammatory responses, HEK293T cells were transfected with Rv1804c-encoding plasmids.

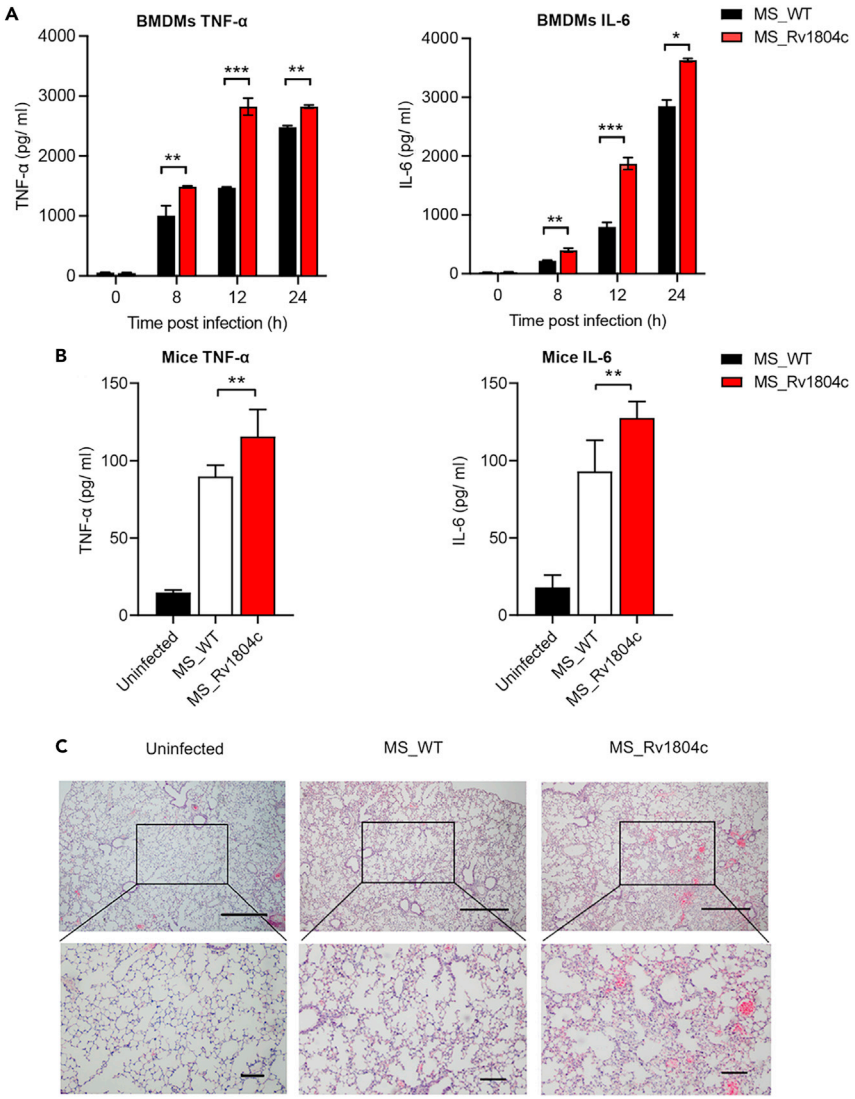

Figure 3. Exogenous Rv1804c expression in *Mycobacterium smegmatis* (*MS*) promotes inflammatory responses

(A) ELISA to quantify the levels of TNF-α and IL-6 in the supernatants of BMDMs infected with *MS_WT* and *MS_Rv1804c* at an MOI of 10 for 0, 8, 12, and 24 h.

(B) ELISA to quantify the levels of TNF-α and IL-6 in the lung tissues of mice infected with *MS_WT* and *MS_Rv1804c* (2×10^7 CFU/mice) for 6 days.

(C) Hematoxylin and eosin staining of the lung tissues of the infected mice. Scale bars: 1,000 μm (top; original magnification, ×40) and 200 μm (bottom; original magnification, ×100). Data are presented as means ± SD. **p < 0.01 and ***p < 0.001.

The NF-κB luciferase reporter assay revealed that Rv1804c can activate the expression of the NF-κB reporter gene (Figure 5A). Furthermore, *ΔRv1804c*-infected macrophages had lower p-NF-κB p65 expression than *ΔRv1804c+Rv1804c* and control *BCG* in BMDMs (Figure 5B) and RAW264.7 cells (Figure S4A). In addition, the expression of phosphorylated NF-κB p65 (p-NF-κB p65) was increased in *MS_Rv1804c*-infected BMDMs (Figure 5C) and RAW264.7 cells (Figure S4B) compared with *MS_WT*. The enhancement of Rv1804c-mediated inflammatory responses was diminished using the NF-κB inhibitor JSH-23 but not the MAPK inhibitors adezmapimod (p38 inhibitor, 10 μM), SP600125 (JNK inhibitor, 10 μM), and PD98059 (ERK inhibitor, 50 μM) (Figure 5D). This suggests that Rv1804c promotes inflammatory response via the NF-κB pathway. Taken together, the aforementioned results suggest that *Mtb* Rv1804c promotes inflammatory responses via the NF-κB pathway.

Rv1804c promotes NF-κB activation in an IKKα-independent manner

The activated IκBα kinase complex IKK specifically phosphorylates IκBα, resulting in the degradation of IκBα and nuclear translocation of NF-κB in *Mtb*-infected macrophages.[28] To evaluate whether Rv1804c promotes the activation of the NF-κB pathway by affecting the activity of the IKK complex, BMDMs and RAW264.7 cells were infected with *ΔRv1804c*, *ΔRv1804c+Rv1804c*, and control *BCG*. The expression of *p*-IKKα in *ΔRv1804c*-infected BMDMs (Figure 6A) and RAW264.7 cells (Figure S4C) was similar to that in *BCG* and *ΔRv1804c+Rv1804c*-infected cells.

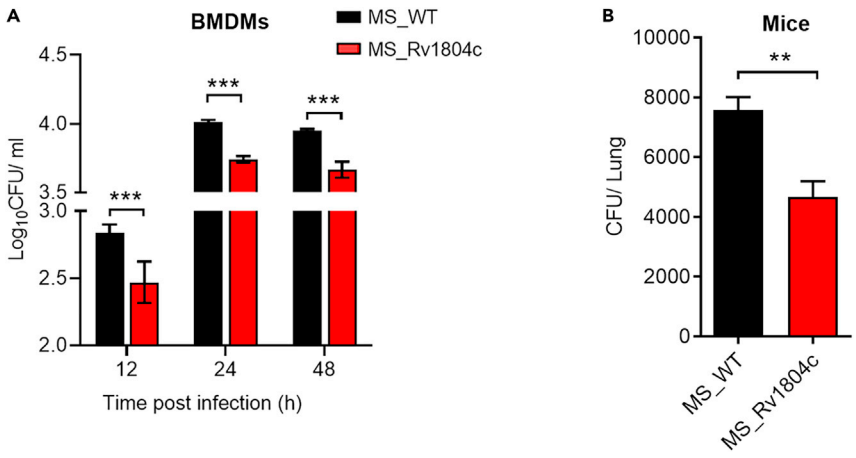

Figure 4. Exogenous Rv1804c expression in *MS* inhibits mycobacterial survival

(A) CFU assay of BMDMs infected with *MS_WT* and *MS_Rv1804c* at an MOI of 20 for 12, 24, and 48 h.

(B) CFU assay of the lung tissues of mice infected with *MS_WT* and *MS_Rv1804c* (2×10^7 CFU/mice) for 6 days. Data are presented as means ± SD. *p < 0.01, **p < 0.01, and ***p < 0.001.

This finding suggests that Rv1804c promotes NF-κB activation in an IKKα-independent manner. TLR2 and TLR4 are important receptors for recognizing *Mtb* infection.[6,29] Moreover, *MS_Rv1804c* infection still increased inflammatory cytokine levels (TNF-α and IL-6) in $TLR2^{-/-}$ and $TLR4^{-/-}$ BMDMs (Figure 6B) indicating that TLR2 and TLR4 are not essential for Rv1804c-promoted inflammatory response activation.

Rv1804c interacts with IκBα via the PEST domain

The activation of the TLR signaling pathway upon *Mtb* infection can induce the expression of inflammatory cytokines.[29] We explored the interactions between Rv1804c and key molecules in the TLR signaling pathway. Interestingly, IκBα, a molecule downstream of the IKK complex, and TGF-β-activated kinase 1 (TAK1), a molecule upstream of the IKK complex, were both coimmunoprecipitated with Rv1804c. The NF-κB luciferase reporter assay revealed that the enhancement of Rv1804c-mediated inflammatory responses was diminished using the IκBα phosphorylation inhibitor BAY-11–7085 (5 μM) but not the TAK1 inhibitor OZ (1 μM) (data not shown). This suggests that Rv1804c promotes NF-κB activation by interacting with IκBα. Immunoprecipitation experiments revealed that Rv1804c interacts with exogenous IκBα (Figure 7A). Furthermore, the *in vitro* precipitation assay revealed that purified Rv1804c can directly interact with endogenous IκBα in RAW264.7 cells (Figure 7B). In addition, immunoprecipitation and confocal microscopy revealed that Rv1804c interacts or colocalizes with endogenous IκBα in both HEK293T (Figures 7C and 7D) and RAW264.7 (Figures 7E and 7F) cells.

Murine IκBα has three conserved domains and comprises 317 amino acids, including the N-terminal signal receiving domain (1–72 amino acids), intermediate anchor repeat domain (73–280 amino acids), and C-terminal PEST domain (281–317 amino acids), with a total molecular weight of 36 kDa.[30] Next, to identify the potential IκBα domain that interacts with Rv1804c, IκBα was split into three truncated mutants: IκBαΔPEST (Fragment 1, F1), IκBαΔSRD and PEST (Fragment 2, F2), and IκBαΔSRD (Fragment 3, F3) (Figure 7G). Immunoprecipitation experiments revealed that Rv1804c interacts with the F3 but not with F1 and F2. This indicates that Rv1804c interacts with IκBα via the PEST domain (Figure 7H).

Rv1804c increases IκBα phosphorylation

We determined whether Rv1804c affects IκBα. HEK293T and RAW264.7 cells were transfected with Rv1804c-encoding plasmids, followed by the measurement of IκBα phosphorylation. Western blotting revealed that Rv1804c overexpression markedly enhanced IκBα phosphorylation in TNF-α-stimulated HEK293T cells (Figure 8A) and *BCG*-infected RAW264.7 cells (Figure 8B). And the expression of p-NF-κB p65 and *p*-IκBα decreased in *ΔRv1804c*-infected RAW264.7 cells compared with *ΔRv1804c+Rv1804c*-infected cells (Figure 8C). This suggests that Rv1804c increases IκBα phosphorylation in *Mtb*-infected macrophages. Phosphorylated IκBα is generally degraded via the ubiquitin-proteasome pathway, which is mediated by the E3 ubiquitin ligase β-TrCP.[31] Western blotting revealed that IκBα levels increased in Rv1804c-overexpressing cells in the presence of the proteasome inhibitor MG132 (Figure 8D), indicating that the ubiquitin-protease degradation system was involved in Rv1804c-induced IκBα reduction. In line with this, an intense ubiquitinated IκBα ladder was observed in Rv1804c-overexpressing 293T cells compared with control cells (Figure 8E). Taken together, these findings suggest that Rv1804c increases IκBα phosphorylation and that phosphorylated IκBα is degraded via the ubiquitin-protease-dependent pathway.

Rv1804c is not enriched in virulent but in attenuated mycobacterium and is related to clinical TB

The expression of *Mtb* proteins varies among different strains and is associated with clinical disease progression.[32,33] qPCR was performed to evaluate Rv1804c expression in *BCG*, *Mtb H37Rv*, and 13 *Mtb* clinical isolates. Rv1804c expression was markedly lower in the virulent *H37Rv*

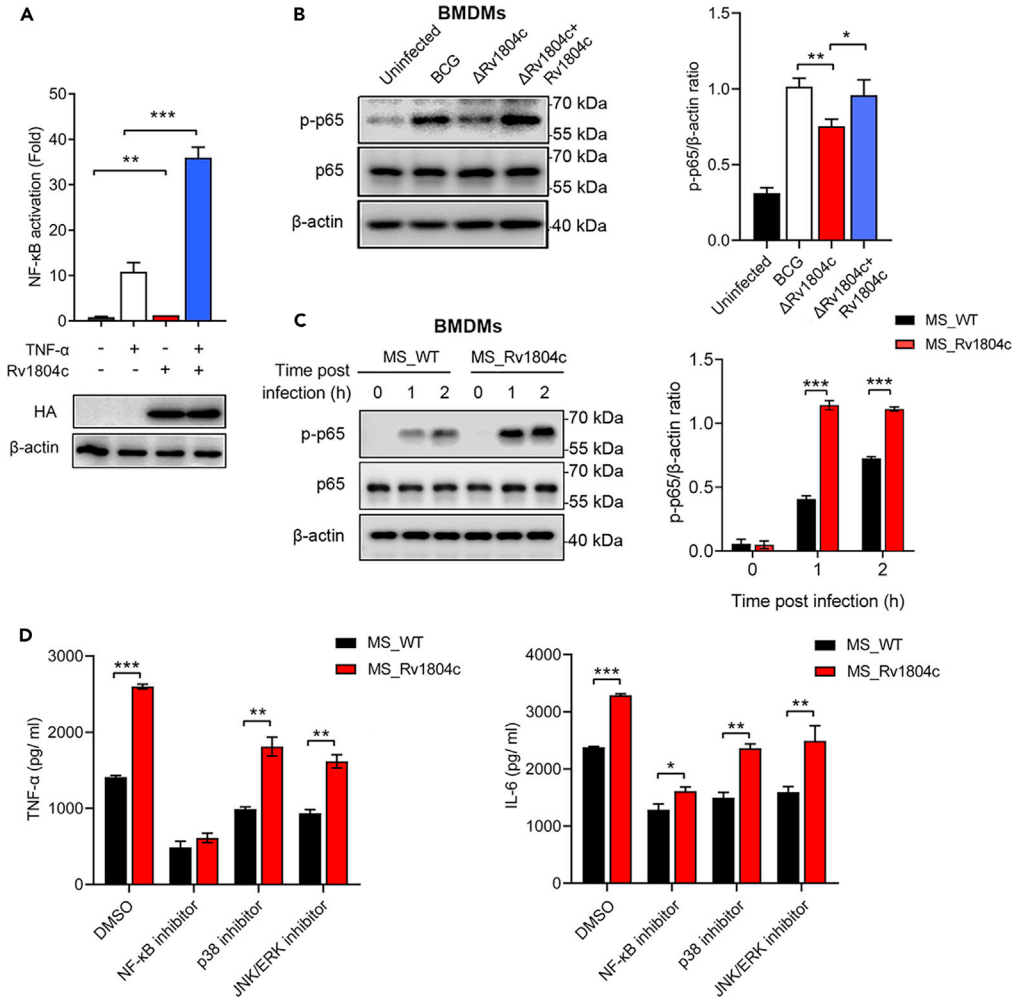

Figure 5. Rv1804c promotes inflammatory responses via the NF-κB pathway

(A) Immunoblotting and NF-κB luciferase reporter assay of HEK293T cells transfected with the HA-Rv1804c plasmid along with pRL-TK and pNF-κB for 24 h.

(B) Immunoblotting of p-NF-κB p65 and NF-κB p65 in BMDMs infected with *BCG*, *ΔRv1804c*, and *ΔRv1804c+Rv1804c* at an MOI of 10 for 1 h.

(C) Immunoblotting of p-NF-κB p65 and NF-κB p65 in and BMDMs infected with *MS_WT* and *MS_Rv1804c* at an MOI of 10 for 1 and 2 h.

(D) ELISA to quantify the levels of TNF-α and IL-6 in the supernatants of RAW264.7 cells pretreated with NF-κB, p38, and JNK/ERK inhibitors for 1 h. Densitometric quantification of the western blotting results was performed using ImageJ. Data are presented as means ± SD. *p < 0.01, **p < 0.01, and ***p < 0.001.

strain than in *BCG*; furthermore, it decreased in all 13 clinical isolates (Figure 9A). Two RNA polymerase (rpoB) probes (probe A and probe B) were used in the GeneXpert PCR assays to measure the amounts of *Mtb* in sputum or bronchoalveolar lavage fluid; the CT values were used to indirectly reflect sputum bacterial loads. The higher the bacterial load in the sputum, the lower the GeneXpert CT value. Interestingly, we observed that Rv1804c expression was positively correlated with GeneXpert CT values (Figure 9B). This indicates that Rv1804c expression in the clinical isolates is negatively correlated with the bacterial loads in patients with *Mtb* infection. Taken together, these data suggest that Rv1804c plays an important role in *Mtb* infection and TB progression.

DISCUSSION

The sequencing of the whole genome of *Mtb* is a milestone marking the entry of *Mtb* research into the post-genomic stage.[33] Many *Mtb* genes, including those encoding secretory proteins such as CFP10, ESAT-6, and LpqH, are related to the virulence of *Mtb*.[10,34,35] However, the mechanism by which *Mtb* secretory proteins participate in immune regulation remains unknown. *Mtb* Rv1804c, a predicted and conserved *Mtb* secretory protein identified in the culture filtrates of *Mtb H37Rv*, is a nonessential gene for the *in vitro* growth of *H37Rv* via Himar1 transposon mutagenesis; it may be a link between innate immunity and autophagy.[20–22] In the present study, Rv1804c knockdown in *BCG* led to the decreased expression of inflammatory cytokines and alleviated tissue damage in the lungs of infected mice. Therefore, Rv1804c may be a factor promoting *Mtb*-induced host immune responses, indicating a potential mechanism underlying the function of *Mtb* secretory proteins.

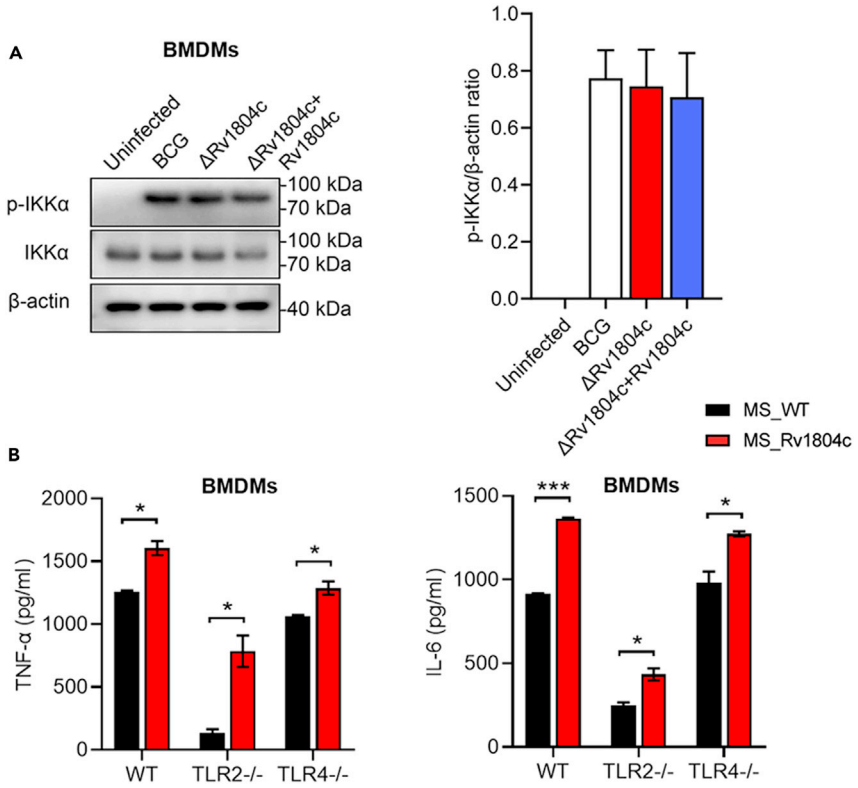

Figure 6. Rv1804c promotes NF-κB activation via an IKKα-independent manner

(A) Immunoblotting of *p*-IKKα and IKKα in BMDMs infected with *BCG*, *ΔRv1804c*, and *ΔRv1804c+Rv1804c* at an MOI of 10 for 1 h. Densitometric quantification of western blotting results was performed using ImageJ.

(B) ELISA to quantify the levels of TNF-α and IL-6 in the supernatants of TLR2$^{-/-}$ and TLR4$^{-/-}$ BMDMs infected with *MS_WT* and *MS_Rv1804c* at an MOI of 10 for 12 h. Data are presented as means ± SD. *p < 0.01.

Specific molecular patterns associated with bacterial components are recognized by host receptors located on the membrane or in the cytosol; this leads to the downstream activation of the NF-κB and MAPK pathways[6] For example, the *Mtb* protein EsxL induces TNF-α production via the TLR2-dependent activation of the MAPK and NF-κB pathways.[17] Similarly, another *Mtb* secretory protein, MPT83, activates the MAPK signaling pathway via the TLR2 pathway, thereby promoting cytokine production and apoptosis.[36] However, information on the *Mtb* secretory proteins recognized by host receptor-independent pathways to initiate immune responses is lacking. In the present study, we observed that Rv1804c promotes inflammatory responses primarily via the NF-κB pathway and not the MAPK pathway. Including TNF-α and IL-6, we also found that the levels of IL-1β, IL-12, and NO but not IL-10 increased in the supernatants of *MS_Rv1804c* infected RAW264.7 cells or mice lung tissues, again confirming that Rv1804 enhances the inflammatory responses (Figure S5). In the classical NF-κB signaling pathways, adaptor proteins such as TRAF6, TAB1, and TAK1 are recruited upon TLR stimulation, resulting in the activation of the IKK complex. The IKK complex further phosphorylates IκBα, resulting in the degradation of IκBα via proteases.[37] Interestingly, we observed that Rv1804c increases IκBα phosphorylation in an IKKα-independent manner. While exploring the underlying mechanisms, we observed that Rv1804c directly interacts with the PEST domain of IκBα. Similar to the findings of our study, several studies have reported that *Mtb* can manipulate the regulatory machinery of immune responses in the host by directly interacting with immune components.[13,38,39] Several kinases, such as IKKβ, casein kinase 2, and Syk,[40] can phosphorylate IκBα. However, no analogous functional kinase domain was predicted in Rv1804c by searching the NCBI database; therefore, we hypothesize that Rv1804c indirectly promotes IκBα phosphorylation. Although there is no evidence, we believe that Rv1804c acts as a bridge between IκBα and an unknown kinase, recruits the kinase, and localizes it to the PEST domain of IκBα, thereby increasing the binding capacity of IκBα to the kinase. Nevertheless, the specific mechanism should be further explored.

It seems very interesting that *Mtb* encode Rv1084, such a gene to promote host inflammatory response, which may initially appear disadvantageous for bacterial survival. Moreover, Rv1804 is evolutionary conserved because we notice that it exists not only in the ancestral *Mtb* strains, but also in the modern *Mtb* strains, suggesting the importance of the role of Rv0124 in *Mtb* life cycle. Accumulating evidence from multiple studies suggests that *Mtb* can enhance host innate immunity via various own proteins.[8,41,42] Our findings, consistent with other studies, identified a *Mtb* gene that promotes host inflammation response via interaction with IκBα of NF-κB signaling.[43] Why does *Mtb* contain pro-inflammatory proteins that appear to be detrimental to its own growth? The pathogenesis of TB is very complicated and it is vital

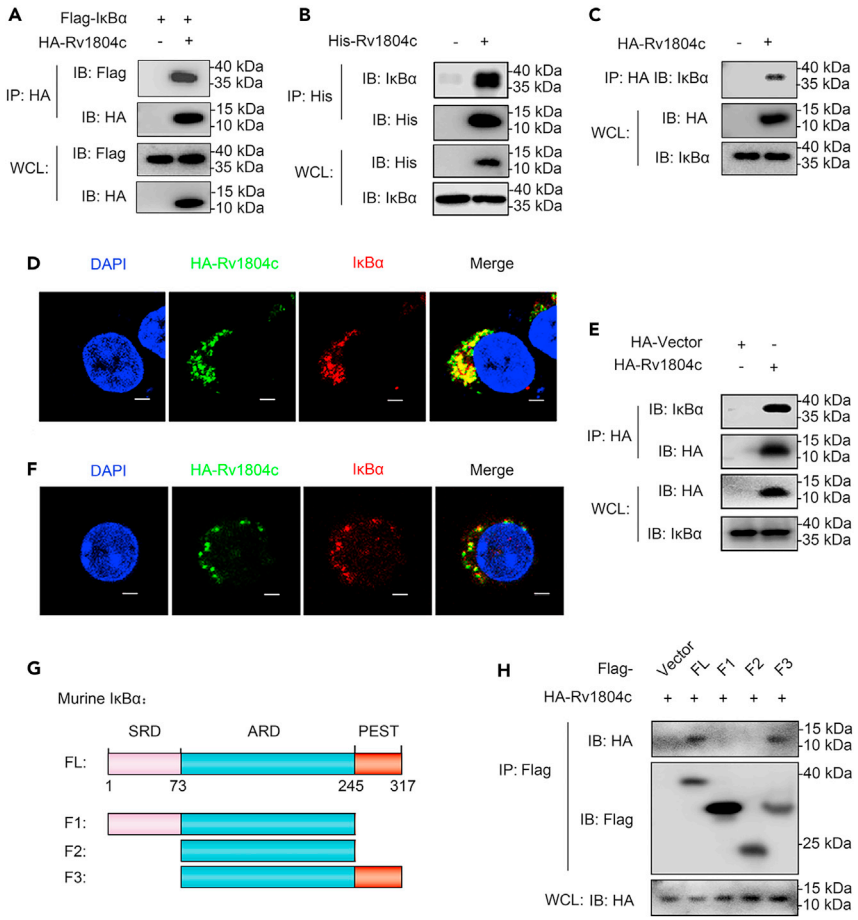

Figure 7. Rv1804c interacts with IκBα via the PEST domain

(A) Immunoblotting and immunoprecipitation assay of the lysates of HEK293T cells transfected with the plasmids HA-Rv1804c and Flag-IκBα.

(B) Precipitation assay of endogenous IκBα in RAW264.7 cells using purified His-Rv1804c.

(C) Immunoblotting and immunoprecipitation assay of the lysates of HEK293T cells transfected with the plasmid HA-Rv1804c.

(D) Immunofluorescence analysis of HEK293T cells transfected with the plasmid HA-Rv1804c Scale bars: 1 μm.

(E) Immunoblotting and immunoprecipitation assay of the lysates of RAW264.7 cells transfected with the plasmid HA-Rv1804c.

(F) Immunofluorescence analysis of RAW264.7 cells transfected with the plasmid HA-Rv1804c. Scale bars: 1 μm.

(G) Schematics of IκBαΔPEST, IκBαΔSRD and PEST, and IκBαΔSRD constructs. FL, full-length; F1, IκBαΔPEST; F2, IκBαΔSRD and PEST; and F3, IκBαΔSRD.

(H) Immunoblotting and immunoprecipitation assay of the lysates of HEK293T cells transfected with relative plasmids. WCL, whole cell lysates; IP, immunoprecipitation; IB, immunoblotting.

for *Mtb* to maintain a balance between host protective and pathogenic immune responses during life cycle.[44] For example, in the early infection of *Mtb*, the inhibition of host immune responses may help the bacteria to better survival in the infected cells. Once the infection is established, the induction of inflammatory cytokines, especially TNF-α is critical for the formation of granulomas,[45] which is a shelter for *Mtb* persistence. Later, an excessive inflammatory response is required to induce the granulomas necrosis, and destruct the lung parenchyma for the better transmission of *Mtb* to the other individuals. In that case, although there is no direct evidence, it is plausible that *Mtb* may utilize its own proteins such as Rv1804c to manipulate host pro-inflammatory responses and create an environment conducive to persistence.

Recently, we reported the differential expression of *Mtb* MmsA and PPE36 between clinical isolates and the standard virulent strain *Mtb* H37Rv.[15,32] Interestingly, in the present study, Rv1804c was highly enriched in the attenuated *BCG* strain than in the virulent *H37Rv* strain. Furthermore, Rv1804c inhibits mycobacterial survival both *in vitro* and *in vivo*.

In conclusion, we identified a novel *Mtb* protein, Rv1804c, that promotes macrophage-mediated inflammatory responses in an IKKα-independent manner. This mechanism is different from the classical NF-κB signaling pathway. The *Mtb* secretory protein Rv1804c directly binds to the PEST domain of IκBα, increasing IκBα phosphorylation and degrading it via the ubiquitin-proteasome pathway during *Mtb* infection. In addition, the levels of Rv1804c in clinical isolates are associated with TB progression. Our study findings provide insights and ideas that *Mtb* secretory proteins are recognized via the host receptor-independent pathway to initiate immune responses and may facilitate the development of more efficient vaccines.

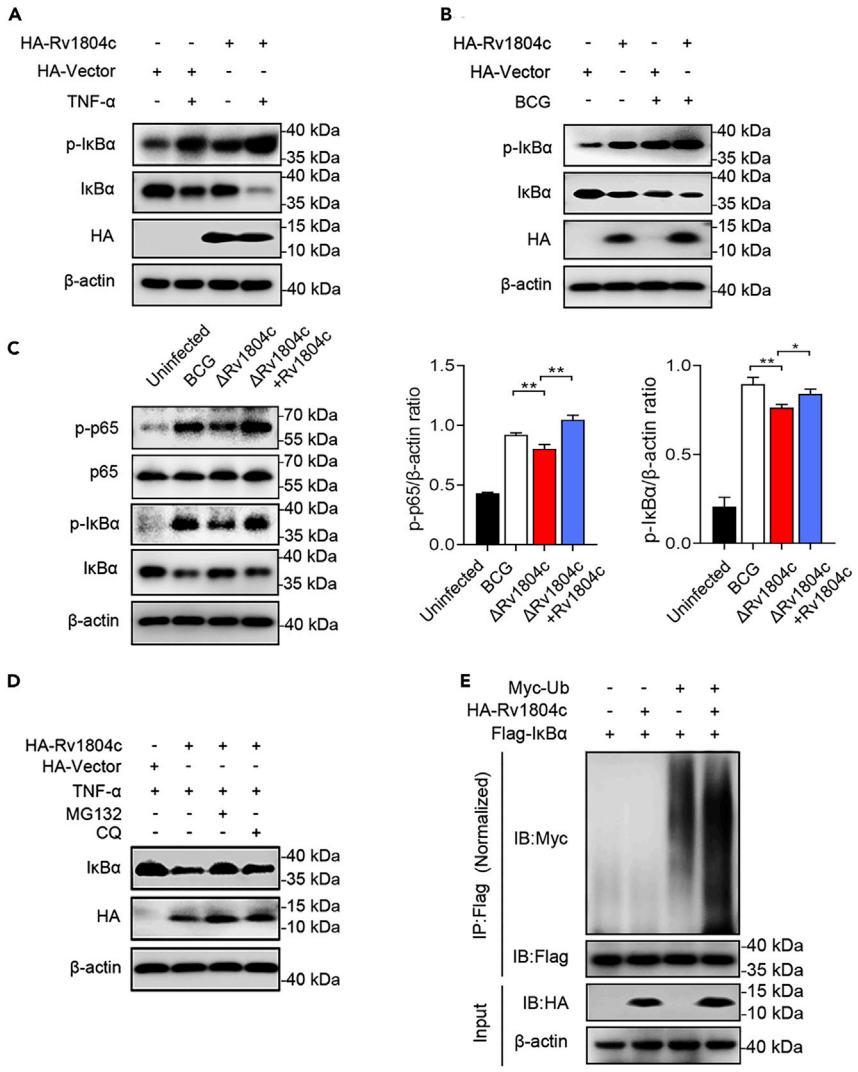

Figure 8. Rv1804c increases IκBα phosphorylation

(A and B) Immunoblotting of *p*-IκBα and IκBα in HEK293T cells transfected with the plasmids HA-Rv1804c (A) or HA-vector after TNF stimulation and RAW264.7 cells infected with *BCG*.

(C) Immunoblotting of p-NF-κB p65, NF-κB p65, *p*-IκBα, and IκBα in RAW264.7 cells infected with *BCG*, *ΔRv1804c*, and *ΔRv1804c+Rv1804c* at an MOI of 10 for 1 h. Densitometric quantification of western blotting results was performed using ImageJ.

(D) Immunoblotting of IκBα in HEK293T cells transfected with HA-Rv1804c in the presence or absence of the proteasome inhibitor MG132 and the autophagy lysosomal fusion inhibitor CQ.

(E) Immunoblotting and immunoprecipitation assay of HEK293T cells cotransfected with Flag-IκBα, Myc-Ub, and HA-Rv1804c/HA-vector. IP, immunoprecipitation; IB, immunoblotting.

Limitations of the study

In the present study, we demonstrate that Rv1804c binds to the PEST domain of IκBα and inhibits *BCG* and *MS* survival by activating macrophage-mediated proinflammatory responses but has some limitations. First, the mechanism by which Rv1804c increases IκBα phosphorylation needs to be investigated further. Second, our study relied on overexpression studies in non-pathogenic *MS* or deletion mutants in attenuated *BCG* strains but lacking *Mtb* strains. We acknowledge potential confounding factors in clinical samples and highlight the need for further clinical validation to strengthen the robustness and generalizability of our findings. Firstly, the sample size of clinical samples in our study needs to be expanded to verify the experimental results. Secondly, the clinical samples in our study come from diverse patient populations with variations in disease stage, treatment history, comorbidities, and genetic background. These factors can introduce variability and potential confounders in the analysis of Rv1804c expression. Further validation in larger cohorts with standardized patient selection criteria would help mitigate the impact of these confounders. Thirdly, while an association between Rv1804c expression and TB progression

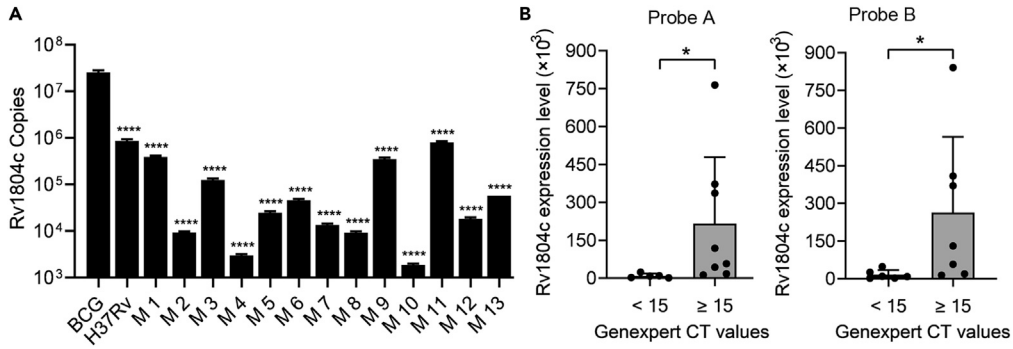

Figure 9. Rv1804c is not enriched in virulent but attenuated mycobacterium and is related to clinical TB

(A) qPCR analysis of Rv1804c in *BCG*, *H37Rv*, and clinical isolates (n = 13).

(B) Rv1804c expression in clinical isolates using the GeneXpert CT values of clinical samples. The median GeneXpert CT value (GeneXpert CT value = 15) was used for grouping.Data are presented as means ± SD. *p < 0.01 and ****p < 0.0001.

or bacterial loads may be observed, it is essential to establish whether Rv1804c expression is a causal factor or simply a biomarker. Further mechanistic studies, such as *in vitro* experiments or animal models of Mtb clinical isolates, can provide insights into the functional role of Rv1804c in TB pathogenesis.

STAR★METHODS

Detailed methods are provided in the online version of this paper and include the following:

- KEY RESOURCES TABLE
- RESOURCE AVAILABILITY
  - Lead contact
  - Materials availability
  - Data and code availability
- EXPERIMENTAL MODEL AND STUDY PARTICIPANT DETAILS
  - Bacterial strains
  - Cell lines
- METHOD DETAILS
  - Plasmids, reagents, and antibodies
  - Construction of the *Mtb* strains
  - *Mtb* culture infiltrate and bacterial lysates separation
  - Transfection
  - Luciferase assay
  - Real-time quantitative polymerase chain reaction (qPCR)
  - Immunoprecipitation and immunoblotting
  - Confocal microscopy
  - Ubiquitination assay
  - Colony-forming unit (CFU) assay
  - GeneXpert assay
- QUANTIFICATION AND STATISTICAL ANALYSIS

SUPPLEMENTAL INFORMATION

Supplemental information can be found online at https://doi.org/10.1016/j.isci.2024.109101.

ACKNOWLEDGMENTS

We thank Prof. Lin Chen and Doctor Zhangli Peng from the Affiliated Hospital of Zunyi Medical University for providing the clinical isolates cDNA for this study. This work was supported by grants from the National Natural Science Foundation of China (31970844, 32170148, 82101848, 32170927, and 82371813), Jiangsu Provincial Innovative Research Team and the Priority Academic Program Development of Jiangsu Higher Education Institutions (PAPD).

AUTHOR CONTRIBUTIONS

J.Z. performed all experiments and analyzed the data. S.X. and C.D. designed the experiments and wrote the manuscript. All authors have given final approval of the version to be published and agree to be accountable for all aspects of the work.

DECLARATION OF INTERESTS

The authors declare no competing interests.

Received: September 30, 2023
Revised: December 18, 2023
Accepted: January 30, 2024
Published: February 6, 2024

REFERENCES

1. Bagcchi, S. (2023). WHO's Global Tuberculosis Report 2022. Lancet Microbe. *4*, e20.
2. Brites, D., and Gagneux, S. (2015). Co-evolution of Mycobacterium tuberculosis and Homo sapiens. Immunol. Rev. *264*, 6–24.
3. Paleckyte, A., Dissanayake, O., Mpagama, S., Lipman, M.C., and McHugh, T.D. (2021). Reducing the risk of tuberculosis transmission for HCWs in high incidence settings. Antimicrob. Resist. Infect. Control *10*, 106.
4. Ahmad, F., Rani, A., Alam, A., Zarin, S., Pandey, S., Singh, H., Hasnain, S.E., and Ehtesham, N.Z. (2022). Macrophage: A Cell With Many Faces and Functions in Tuberculosis. Front. Immunol. *13*, 747799.
5. Hmama, Z., Peña-Díaz, S., Joseph, S., and Av-Gay, Y. (2015). Immunoevasion and immunosuppression of the macrophage by Mycobacterium tuberculosis. Immunol. Rev. *264*, 220–232.
6. Kleinnijenhuis, J., Oosting, M., Joosten, L.A.B., Netea, M.G., and Van Crevel, R. (2011). Innate immune recognition of Mycobacterium tuberculosis. Clin. Dev. Immunol. *2011*, 405310.
7. Brooks, M.N., Rajaram, M.V.S., Azad, A.K., Amer, A.O., Valdivia-Arenas, M.A., Park, J.H., Núñez, G., and Schlesinger, L.S. (2011). NOD2 controls the nature of the inflammatory response and subsequent fate of Mycobacterium tuberculosis and M. bovis BCG in human macrophages. Cell. Microbiol. *13*, 402–418.
8. Liu, C.H., Liu, H., and Ge, B. (2017). Innate immunity in tuberculosis: host defense vs pathogen evasion. Cell. Mol. Immunol. *14*, 963–975.
9. Mishra, B.B., Moura-Alves, P., Sonawane, A., Hacohen, N., Griffiths, G., Moita, L.F., and Anes, E. (2010). Mycobacterium tuberculosis protein ESAT-6 is a potent activator of the NLRP3/ASC inflammasome. Cell. Microbiol. *12*, 1046–1063.
10. Rastogi, S., and Briken, V. (2022). Interaction of Mycobacteria With Host Cell Inflammasomes. Front. Immunol. *13*, 791136.
11. Simeone, R., Sayes, F., Song, O., Gröschel, M.I., Brodin, P., Brosch, R., and Majlessi, L. (2015). Cytosolic access of Mycobacterium tuberculosis: critical impact of phagosomal acidification control and demonstration of occurrence in vivo. PLoS Pathog. *11*, e1004650.
12. Wang, J., Li, B.X., Ge, P.P., Li, J., Wang, Q., Gao, G.F., Qiu, X.B., and Liu, C.H. (2015). Mycobacterium tuberculosis suppresses innate immunity by coopting the host ubiquitin system. Nat. Immunol. *16*, 237–245.
13. Dou, Y., Xie, Y., Zhang, L., Liu, S., Xu, D., Wei, Y., Li, Y., and Zhang, X.L. (2022). Host MKRN1-Mediated Mycobacterial PPE Protein Ubiquitination Suppresses Innate Immune Response. Front. Immunol. *13*, 880315.
14. Wang, L., Wu, J., Li, J., Yang, H., Tang, T., Liang, H., Zuo, M., Wang, J., Liu, H., Liu, F., et al. (2020). Host-mediated ubiquitination of a mycobacterial protein suppresses immunity. Nature *577*, 682–688.
15. Peng, Z., Yue, Y., and Xiong, S. (2022). Mycobacterial PPE36 Modulates Host Inflammation by Promoting E3 Ligase Smurf1-Mediated MyD88 Degradation. Front. Immunol. *13*, 690667.
16. Kim, J.S., Kim, W.S., Choi, H.H., Kim, H.M., Kwon, K.W., Han, S.J., Cha, S.B., Cho, S.N., Koh, W.J., and Shin, S.J. (2015). Mycobacterium tuberculosis MmsA, a novel immunostimulatory antigen, induces dendritic cell activation and promotes Th1 cell-type immune responses. Cell. Immunol. *298*, 115–125.
17. Pattanaik, K.P., Ganguli, G., Naik, S.K., and Sonawane, A. (2021). Mycobacterium tuberculosis EsxL induces TNF-alpha secretion through activation of TLR2 dependent MAPK and NF-kappaB pathways. Mol. Immunol. *130*, 133–141.
18. Cong, Q., Anishchenko, I., Ovchinnikov, S., and Baker, D. (2019). Protein interaction networks revealed by proteome coevolution. Science *365*, 185–189.
19. Low, T.Y., Syafruddin, S.E., Mohtar, M.A., Vellaichamy, A., A Rahman, N.S., Pung, Y.F., and Tan, C.S.H. (2021). Recent progress in mass spectrometry-based strategies for elucidating protein-protein interactions. Cell. Mol. Life Sci. *78*, 5325–5339.
20. Penn, B.H., Netter, Z., Johnson, J.R., Von Dollen, J., Jang, G.M., Johnson, T., Ohol, Y.M., Maher, C., Bell, S.L., Geiger, K., et al. (2018). An Mtb-Human Protein-Protein Interaction Map Identifies a Switch between Host Antiviral and Antibacterial Responses. Mol. Cell *71*, 637–648.e5.
21. Målen, H., Berven, F.S., Fladmark, K.E., and Wiker, H.G. (2007). Comprehensive analysis of exported proteins from Mycobacterium tuberculosis H37Rv. Proteomics *7*, 1702–1718.
22. Minato, Y., Gohl, D.M., Thiede, J.M., Chacón, J.M., Harcombe, W.R., Maruyama, F., and Baughn, A.D. (2019). Genomewide Assessment of Mycobacterium tuberculosis Conditionally Essential Metabolic Pathways. mSystems *4*. e00070–19.
23. Etna, M.P., Giacomini, E., Severa, M., and Coccia, E.M. (2014). Pro- and anti-inflammatory cytokines in tuberculosis: a two-edged sword in TB pathogenesis. Semin. Immunol. *26*, 543–551.
24. Wu, X., Wu, Y., Zheng, R., Tang, F., Qin, L., Lai, D., Zhang, L., Chen, L., Yan, B., Yang, H., et al. (2021). Sensing of mycobacterial arabinogalactan by galectin-9 exacerbates mycobacterial infection. EMBO Rep. *22*, e51678.
25. Hai, H.T., Vinh, D.N., Thu, D.D.A., Hanh, N.T., Phu, N.H., Srinivasan, V., Thwaites, G.E., and T T Thuong, N. (2019). Comparison of the Mycobacterium tuberculosis molecular bacterial load assay, microscopy and GeneXpert versus liquid culture for viable bacterial load quantification before and after starting pulmonary tuberculosis treatment. Tuberculosis (Edinb) *119*, 101864.
26. Liu, T., Zhang, L., Joo, D., and Sun, S.C. (2017). NF-kappaB signaling in inflammation. Signal Transduct. Target. Ther. *2*, 17023.
27. Fallahi-Sichani, M., Kirschner, D.E., and Linderman, J.J. (2012). NF-kappaB Signaling Dynamics Play a Key Role in Infection Control in Tuberculosis. Front. Physiol. *3*, 170.
28. Hinz, M., and Scheidereit, C. (2014). The IkappaB kinase complex in NF-kappaB regulation and beyond. EMBO Rep. *15*, 46–61.
29. Stamm, C.E., Collins, A.C., and Shiloh, M.U. (2015). Sensing of Mycobacterium tuberculosis and consequences to both host and bacillus. Immunol. Rev. *264*, 204–219.
30. Chen, Z.J. (2005). Ubiquitin signalling in the NF-kappaB pathway. Nat. Cell Biol. *7*, 758–765.
31. Karin, M., and Ben-Neriah, Y. (2000). Phosphorylation meets ubiquitination: the control of NF-[kappa]B activity. Annu. Rev. Immunol. *18*, 621–663.
32. Sun, Y., Zhang, W., Dong, C., and Xiong, S. (2020). Mycobacterium tuberculosis MmsA (Rv0753c) Interacts with STING and Blunts the Type I Interferon Response. mBio *11*, e03254-19.
33. Zheng, H., Lu, L., Wang, B., Pu, S., Zhang, X., Zhu, G., Shi, W., Zhang, L., Wang, H., Wang, S., et al. (2008). Genetic basis of virulence attenuation revealed by comparative genomic analysis of Mycobacterium tuberculosis strain H37Ra versus H37Rv. PLoS One *3*, e2375.
34. Pathak, S.K., Basu, S., Basu, K.K., Banerjee, A., Pathak, S., Bhattacharyya, A., Kaisho, T., Kundu, M., and Basu, J. (2007). Direct extracellular interaction between the early secreted antigen ESAT-6 of Mycobacterium tuberculosis and TLR2 inhibits TLR signaling in macrophages. Nat. Immunol. *8*, 610–618.

35. Arend, S.M., Andersen, P., van Meijgaarden, K.E., Skjot, R.L., Subronto, Y.W., van Dissel, J.T., and Ottenhoff, T.H. (2000). Detection of active tuberculosis infection by T cell responses to early-secreted antigenic target 6-kDa protein and culture filtrate protein 10. J. Infect. Dis. *181*, 1850–1854.
36. Wang, L., Zuo, M., Chen, H., Liu, S., Wu, X., Cui, Z., Yang, H., Liu, H., and Ge, B. (2017). Mycobacterium tuberculosis Lipoprotein MPT83 Induces Apoptosis of Infected Macrophages by Activating the TLR2/p38/COX-2 Signaling Pathway. J. Immunol. *198*, 4772–4780.
37. Zhang, Q., Lenardo, M.J., and Baltimore, D. (2017). 30 Years of NF-kappaB: A Blossoming of Relevance to Human Pathobiology. Cell *168*, 37–57.
38. Chaurasiya, S.K., and Srivastava, K.K. (2009). Downregulation of protein kinase C-alpha enhances intracellular survival of Mycobacteria: role of PknG. BMC Microbiol. *9*, 271.
39. Kim, K.H., An, D.R., Song, J., Yoon, J.Y., Kim, H.S., Yoon, H.J., Im, H.N., Kim, J., Kim, D.J., Lee, S.J., et al. (2012). Mycobacterium tuberculosis Eis protein initiates suppression of host immune responses by acetylation of DUSP16/MKP-7. Proc. Natl. Acad. Sci. USA *109*, 7729–7734.
40. Viatour, P., Merville, M.P., Bours, V., and Chariot, A. (2005). Phosphorylation of NF-kappaB and IkappaB proteins: implications in cancer and inflammation. Trends Biochem. Sci. *30*, 43–52.
41. Ernst, J.D. (2012). The immunological life cycle of tuberculosis. Nat. Rev. Immunol. *12*, 581–591.
42. O'Garra, A., Redford, P.S., McNab, F.W., Bloom, C.I., Wilkinson, R.J., and Berry, M.P.R. (2013). The immune response in tuberculosis. Annu. Rev. Immunol. *31*, 475–527.
43. Wang, L., Liu, Z., Wang, J., Liu, H., Wu, J., Tang, T., Li, H., Yang, H., Qin, L., Ma, D., et al. (2019). Oxidization of TGFbeta-activated kinase by MPT53 is required for immunity to Mycobacterium tuberculosis. Nat. Microbiol. *4*, 1378–1388.
44. Orme, I.M., Robinson, R.T., and Cooper, A.M. (2015). The balance between protective and pathogenic immune responses in the TB-infected lung. Nat. Immunol. *16*, 57–63.
45. Cohen, S.B., Gern, B.H., and Urdahl, K.B. (2022). The Tuberculous Granuloma and Preexisting Immunity. Annu. Rev. Immunol. *40*, 589–614.
46. Jordao, L., Bleck, C.K.E., Mayorga, L., Griffiths, G., and Anes, E. (2008). On the killing of mycobacteria by macrophages. Cell. Microbiol. *10*, 529–548.
47. Qiang, L., Wang, J., Zhang, Y., Ge, P., Chai, Q., Li, B., Shi, Y., Zhang, L., Gao, G.F., and Liu, C.H. (2019). Mycobacterium tuberculosis Mce2E suppresses the macrophage innate immune response and promotes epithelial cell proliferation. Cell. Mol. Immunol. *16*, 380–391.
48. Salvador-Martín, S., Raposo-Gutiérrez, I., Navas-López, V.M., Gallego-Fernández, C., Moreno-Álvarez, A., Solar-Boga, A., Muñoz-Codoceo, R., Magallares, L., Martínez-Ojinaga, E., Fobelo, M.J., et al. (2020). Gene Signatures of Early Response to Anti-TNF Drugs in Pediatric Inflammatory Bowel Disease. Int. J. Mol. Sci. *21*, 3364.

STAR★METHODS

KEY RESOURCES TABLE

REAGENT or RESOURCE	SOURCE	IDENTIFIER
Antibodies		
Anti-NF-κB p65	Cell Signaling Technology	Cat# 8242; RRID:AB_10859369
Anti-p-NF-κB p65	Cell Signaling Technology	Cat# 3033; RRID:AB_331284
Anti-IκBα	Cell Signaling Technology	Cat# 9242; RRID:AB_331623
Anti-p-IκBα	Cell Signaling Technology	Cat# 2859; RRID:AB_561111
Anti-IKKα	Cell Signaling Technology	Cat# 2682; RRID:AB_331626
Anti-p-IKKα	Cell Signaling Technology	Cat# 2697; RRID:AB_2079382
Anti-HA	Cell Signaling Technology	Cat# 3724; RRID:AB_1549585
Anti-Myc	Cell Signaling Technology	Cat# 2276; RRID:AB_331783
Anti-His	Cell Signaling Technology	Cat# 12698; RRID:AB_2744546
Anti-GroEL	Abcam	Cat# ab82592; RRID:AB_1658428
Anti-β-actin	Cell Signaling Technology	Cat# 3700; RRID:AB_2242334
Anti-Flag	Sigma-Aldrich	Cat# F7425; RRID:AB_439687
HRP-conjugated goat anti-mouse IgG	Southern-Biotech	Cat# 1091-05; RRID:AB_2736842
HRP-conjugated goat anti-rabbit IgG	Southern-Biotech	Cat# 4030-05; RRID:AB_2687483
Anti-Rv1804c	This paper	N/A
DyLight 647-labeled antibody to rabbit IgG	Jackson	Cat# 111-605-144; RRID:AB_2338078
DyLight 488-labeled antibody to mouse IgG	Jackson	Cat# 111-545-003; RRID:AB_2338046
Bacterial and virus strains		
DH5α	weidibio	Cat# DL1001
BL21(DE3)	weidibio	Cat# EC1002S
mc^2 155	Soochow University, China	N/A
BCG WT	Gene Optimal Inc.	N/A
BCG ΔRv1804c	Gene Optimal Inc.	N/A
BCG ΔRv1804c+Rv1804c	Gene Optimal Inc.	N/A
Chemicals and recombinant proteins		
MG132	Selleck	Cat# S3619
JSH-23	MCE	Cat# HY-13982
adezmapimod	MCE	Cat# HY-10256
SP600125	MCE	Cat# HY-12041
PD98059	MCE	Cat# HY-12028
(5Z)-7-oxozeaenol	Sigma	Cat# O9890
BAY-11–7085	MCE	Cat# HY-10257
TRIzol reagent	TAKARA	Cat# 9109
Critical commercial assays		
TNF-α Mouse ELISA Kit	Invitrogen	Cat# 88-7324-88
IL-6 Mouse ELISA Kit	Invitrogen	Cat# 88-7064-88
SYBR Green PCR Master Mix	Vazyme,	Cat# Q331-AA
dual-luciferase reporter assay system	Promega	Cat# E1500
Lipofectamine™ 2000 Transfection Reagent	Invitrogen	Cat# 11668019
RIPA lysis buffer	Beyotime	Cat# P0013B
Anti-FLAG M2 affinity gel	Sigma	Cat# A2220

(*Continued on next page*)

Continued

REAGENT or RESOURCE	SOURCE	IDENTIFIER
Anti-His affinity resin	GenScript Biotech	Cat# L00439
Experimental models: Cell lines		
HEK293T	American Type Culture Collection	N/A
RAW264.7	American Type Culture Collection	N/A
Experimental models: Organisms/strains		
C57BL/6 mice	Experimental Animal Center of the Chinese Academy of Sciences	N/A
Deposited		
Raw western blot	Mendeley Data	https://doi.org/10.17632/6zr5mv7w22.2
Raw H&E	Mendeley Data	
Other		
Others related to the research	This paper	sdxiong@suda.edu.cn

RESOURCE AVAILABILITY

Lead contact

Further information and requests for resources should contact to Prof. Sidong Xiong (sdxiong@suda.edu.cn).

Materials availability

The materials are available upon request.

Data and code availability

- Original western blot and HE images have been deposited at Mendeley and are publicly available as of the date of publication. The DOI is listed in the key resources table. Microscopy data reported in this paper will be shared by the lead contact upon request.
- This paper does not report original code.
- Any additional information required to reanalyze the data reported in this paper is available from the lead contact upon request.

EXPERIMENTAL MODEL AND STUDY PARTICIPANT DETAILS

Bacterial strains

The *Escherichia coli* strains *DH5α* and *BL21* were grown in flasks containing Luria-Bertani medium. The antibiotic ampicillin or kanamycin was added at a concentration of 50 μg/mL for selection. The *Mycobacterium smegmatis* (*MS*) strain *mc²155* was grown in Luria–Bertani medium supplemented with 0.05% Tween 80 (Sigma). *BCG WT* (*BCG*), *BCG ΔRv1804c* (*ΔRv1804c*), and *BCG ΔRv1804c+Rv1804c* (*ΔRv1804c+Rv1804c*) were purchased from Gene Optimal Inc. (Shanghai, China) and grown in Middlebrook 7H9 broth (Becton Dickinson) supplemented with 10% oleic acid–albumin-glucose-catalase (OADC, Sigma) and 0.05% Tween 80 or Middlebrook 7H10 agar (Becton Dickinson) supplemented with 10% OADC. *MS_Rv1804c* and control *MS_WT* were generated at our lab. Plasmids pMV261-Rv1804c and empty vector pMV261 were electroporated into *MS* strain *mc²155*, generating MS_Rv1804c and MS_WT after kanamycin (50 μg/mL) selection, respectively.

Cell lines

HEK293T and RAW264.7 cells were cultured in Dulbecco's modified Eagle medium (HyClone) supplemented with 10% fetal bovine serum (HyClone), 0.1 mg/mL streptomycin (Invitrogen), and 100 U/mL penicillin (Invitrogen) at 37°C under a 5% CO_2 atmosphere. Bone marrow-derived macrophages (BMDMs) were prepared using a previously described method.[15] The cDNAs of *H37Rv* and clinical isolates were obtained from the Affiliated Hospital of Zunyi Medical University in China.

Mouse strains and infection

The animal study was reviewed and approved by the ethics committee of Soochow University. Six-to-eight-week-old female C57BL/6 mice were purchased from the Experimental Animal Center of the Chinese Academy of Sciences (Shanghai, China) and maintained under specific pathogen-free conditions. All experimental procedures involving animals were performed according to the guidelines for the Care and Use of Laboratory Animals (Ministry of Health, China, 1998). The protocols were approved by the ethics committee of Soochow University. For macrophage separations, 6-week-old female mice were used as described previously.[46]

BMDMs or RAW264.7 cells were infected with *MS_WT* and *MS_Rv1804c* at an MOI of 20 or with *BCG*, *ΔRv1804c*, and *ΔRv1804c+Rv1804c* at an MOI of 10. For mice infection, 6-week-old female mice were intranasally infected with approximately 2×10^7 *MS_WT* and *MS_Rv1804c* or 1×10^7 *BCG*, *ΔRv1804c*, and *ΔRv1804c+Rv1804c*.

METHOD DETAILS

Plasmids, reagents, and antibodies

The plasmids pRv1804c-HA, pIκBα-Flag (FL), pIκBα-F1-Flag (F1), pIκBα-F2-Flag (F2), and pIκBα-F3-Flag (F3) were constructed at our laboratory using specific primers. The plasmid encoding *p*-ubiquitin-Myc was provided by Prof. Hui Zheng (Soochow University, China). Furthermore, pNF-kB-luc and pRL-TK, dual-luciferase reporter assay vectors, were purchased from Clontech (Mountain View, CA, USA).

The primary antibodies used were anti-NF-κB p65 (CST, 8242), anti-phosphorylated-NF-κB p65 (p- NF-κB p65, CST, 3033), anti-IκBα (9242, CST), anti-*p*-IκBα (2859, CST), anti-HA (3724, CST), anti-His (CST, 12698), anti-IKKα (CST, 2682), anti-phosphorylated IKKα (*p*-IKKα, CST, 2697), anti-GroEL (Abcam, ab82592), and anti-β-actin (CST, 3700). The secondary antibody used was horseradish peroxidase (HRP)-conjugated goat anti-mouse IgG (Southern-Biotech, 1091–05) and HRP-conjugated goat anti-rabbit IgG (Southern-Biotech, 4030–05). In addition, the inhibitors used were JSH-23 (MCE, HY-13982), adezmapimod (MCE, HY-10256), SP600125 (MCE, HY-12041), PD98059 (MCE, HY-12028), (5Z)-7-oxozeaenol (OZ; Sigma, O9890), and BAY-11–7085 (MCE, HY-10257). Monoclonal mouse anti-HA agarose (SAE0197) was purchased from Sigma.

Construction of the *Mtb* strains

The plasmid pMV261-Rv1804c and empty vector pMV261 were electroporated into the *MS* strain mc^2 155. Clones were obtained after kanamycin (50 μg/mL) selection. The expression of Rv1804c in *MS* was examined via immunoblotting using the anti-Flag antibody. In addition, the expression of Rv1804c in *BCG*, *ΔRv1804c*, and *ΔRv1804c+Rv1804c* was examined using an anti-Rv1804c polyclonal antibody prepared at our lab.

Mtb culture infiltrate and bacterial lysates separation

Bacterial cultures were centrifuged at 3,000 × g for 5 min. Culture filtrates were obtained as supernatants and concentrated using filters with a 3-kD cutoff (Millipore, UFC5003). Cell lysates were obtained by ultrasonicating. The expression of Rv1804c protein in each component was detected by western blotting using a specific antibody prepared in our laboratory. GroEL was used as a cytosol marker control.

Transfection

Lipofectamine 2000 (Invitrogen, 11668019) was used to transfect HEK293T cells, whereas the LipoMax reagent (SUDGEN, 32012) was used to transfect RAW264.7 cells.

Luciferase assay

First, HEK293T cells were cotransfected with pRL-TK (50 ng) and pNF-κB-luc (1 μg) plasmids in the presence of HA-Rv1804c (1 μg) or HA-vector plasmids (1 μg) for 24 h. Thereafter, the cells were treated with TNF-α (20 ng/mL) for 12 h. The dual-luciferase reporter assay system (Promega, E1500) was used to measure luciferase activity.

Real-time quantitative polymerase chain reaction (qPCR)

RNA preparation and qPCR analysis were performed using a previously described method.[47] Gene expression was analyzed using the $2^{-\Delta\Delta CT}$ method.[48] Primers used for qPCR analysis as follows: Mouse TNF-α: (forward: 5′-CTTCTCGAACCCCGAGTGA-3′; reverse: 5′-CCTCTGATGGCACCACCA-3′). Mouse IL-6: (forward: 5′-AGGAGACTTGCCTGGTGAAA-3′; reverse: 5′-CAGGGGTG GT TATTGCATCT-3′). Mouse β-actin: (forward: 5′-AACAGTCCGCCTAGAAGCAC-3′; reverse: 5′-CGTTGACATCCGTAAAGACC-3′).

Immunoprecipitation and immunoblotting

Immunoprecipitation and immunoblotting were performed using a previously described method.[43] Briefly, HEK293T cells were cotransfected with the indicated plasmids. After 48 h, the cells were lysed with Western and IP cell lysis buffer (Beyotime, P0013) supplemented with a 1% protease inhibitor cocktail (Sigma, 539133). Thereafter, the cells were centrifuged to remove debris, and the cell lysates were incubated with anti-FLAG M2 affinity gel (Sigma, A2220) overnight at 4°C. For endogenous immunoprecipitation, the plasmid HA-Rv1804c was transfected into HEK293T cells, followed by cell lysis. Thereafter, the lysate was incubated with anti-FLAG M2 affinity gel at 4°C. In addition, RAW264.7 cell lysates were incubated with rRv1804c containing His-Tag with the anti-His affinity resin (GenScript Biotech, L00439) at 4°C. Samples were centrifuged, washed three times with the cell lysis buffer, and boiled with sodium dodecyl sulfate (SDS) loading buffer.

After separation via SDS–polyacrylamide gel electrophoresis, equal amounts of proteins were electroblotted onto nitrocellulose membranes. Then, the membranes were blocked, incubated with the primary antibody, and washed three times before incubation with the secondary antibody. Signals were detected using an enhanced chemiluminescence kit (Thermo Pierce, Rockford, Illinois, USA) with the Amersham Imager 600 (AI600; GE Healthcare) and quantified using ImageJ software (version 1.6.0_20).

Confocal microscopy

HEK293T and RAW264.7 cells were transfected with HA-Rv1804c. Cells were fixed with 4% formaldehyde and then permeabilized with 0.1% Triton X-100 (Sigma, T9284) in phosphate-buffered saline (PBS) for 30 min at room temperature. The sample was blocked with 3% bovine serum albumin (Sigma, A7030) in PBS for 30 min at 37°C and then incubated with mouse anti-HA and rabbit anti-IκBα overnight at 4°C. After washing the cells three times, they were incubated with DyLight 647-labeled antibody to rabbit IgG (Jackson, 111-605-144) and DyLight 488-labeled antibody to mouse IgG (Jackson, 111-545-003). The cells were examined under a confocal microscope (Nikon A1) equipped with analytical software.

Ubiquitination assay

HEK293T cells were cotransfected with Myc-ubiquitin (50 ng), HA-Rv1804c (1.5 μg), and Flag-IκBα (0.5 μg) for 48 h. Thereafter, cell lysates were prepared. IκBα was immunoprecipitated, and the ubiquitinated IκBα was detected via immunoblotting using HA-specific antibodies (Sigma).

Colony-forming unit (CFU) assay

MS and *BCG* colony-forming unit (CFU) assay and mycobacterial survival detection were performed as described previously.[15] RAW264.7 and BMDMs cells were seeded in 6-well plates and then infected with *BCG* or *MS* for 4 h. Then, cells were washed with fresh medium and treated with 200 μg/mL amikacin for 1 h to kill extracellular bacteria. Afterward, infected cells were lysed with 1 mL sterile water containing 0.05% Triton X-100. For CFU assay, 50 μL cell lysates was plated on the 7H10 or LB medium containing hygromycin and cultured at 37°C.

CFU counting was applied to determine the bacterial burden of murine lung tissues. Homogenized lung tissues were diluted with PBS. In addition, 50 μL of cell lysates or tissue homogenates was added to 7H10 or LB plates, cultured for 4 weeks, and then CFU counting was performed.

GeneXpert assay

GeneXpert assays were used to detect bacterial loads in the clinical sputum and BALF samples as described.[25] In brief, 1 mL sputum or 200 μL BALF decontaminated samples was added into 2 mL of sample reagent and transferred into cartridge. The cartridge then was inserted into the test platform of the GeneXpert instrument (Cepheid).

QUANTIFICATION AND STATISTICAL ANALYSIS

Experiments were performed 3 times, all data are represented as mean ± SD. Statistical differences in 2 groups or more than 2 groups were respectively assessed by Student's *t* test or one-way ANOVA followed by Bonferroni test using GraphPad Prism version 5.0 (GraphPad Software Incorporated, San Diego, CA, USA). A p value of <0.05 was considered statistically significant.